



Investigation of the effects of glycerol addition on the morphology and structural properties of Gd/Er co-doped hydroxyapatite

Bast Ahmed Mohammed ^a, Tankut Ates ^{b,*}, Bahroz Kareem Mahmood ^c, Rebaz Obaid Kareem ^c, Serhat Keser ^d, Niyazi Bulut ^e, Omer Kaygili ^e

^a Department of Applied Physics, College of Science, Charmo University, Chamchamal, Iraq

^b Department of Engineering Basic Sciences, Faculty of Engineering and Natural Sciences, Malatya Turgut Özal University, Battalgazi, Malatya, Türkiye

^c Physics Department, College of Science, University of Halabja, 46018, Halabja, Iraq

^d Department of Chemical Technology, EOSB Higher Vocational School, Firat University, 23119, Elazig, Türkiye

^e Department of Physics, Faculty of Science, Firat University, 23119 Elazig, Türkiye

* Corresponding author: E-mail: tankut.ates@ozal.edu.tr

ABSTRACT

This study investigates the effects of increasing amounts of glycerol, ranging from 0 to 16 mL, used in the synthesis on the structural properties of Gd and Er-based hydroxyapatite (HAp). The samples were prepared via a wet chemical route, and their characterizations were carried out using X-ray diffraction (XRD), Fourier transform infrared (FTIR), scanning electron microscopy (SEM), and energy dispersive X-ray (EDX) spectroscopy. The XRD and FTIR results confirmed the formation of the HAp phase in the samples. It was observed that the addition of glycerol at different amounts in the synthesis affected the crystallinity degree and crystallite size. The morphology was almost not affected by the glycerol content as used.

ARTICLE INFO

Keywords:

Hydroxyapatite,
Glycerol,
X-ray diffraction,
Scanning electron microscopy

Received: 2024-03-26

Accepted: 2024-04-16

ISSN: 2651-3080

DOI: 10.54565/jphcfum.1458970

1. Introduction

Hydroxyapatite (HAp), found in the structure of bones and teeth, is virtually identical to the inorganic component found in these hard tissues. Calcium phosphate is the component that makes up this material, which has a wide range of applications, including dental and orthopedic implants and prostheses. HAp is a chemical that is capable of providing benefits and is appropriate for procedures that include the recovery of hard tissues [1-3]. It is frequently utilized in applications within the field of biomedical science because it possesses properties such as high bioactivity, thermal stability, excellent biocompatibility, and non-toxic behavior [4, 5]. Additionally, HAp can interchange its ions with other foreign ions, which has the potential to improve the biocompatibility, mechanical properties, and microstructure of the material. HAp is represented by the

chemical formula $\text{Ca}_{10}(\text{PO}_4)_6(\text{OH})_2$, and its molar ratio of calcium to phosphorus (Ca:P) is 1.67 [3, 4, 6].

Synthetic HAp crystal structures may be either monoclinic or hexagonal [2, 4, 7, 8]. Lattice constants for the hexagonal HAp are $a = 0.9418$ nm, $b = 0.9418$ nm, and $c = 0.6884$ nm, and $\alpha = \beta = 90^\circ$, and $\gamma = 120^\circ$ [4, 9].

Because it possesses limited mechanical qualities, it appears to be hard to employ HAp as an implant material in the medical industry. To provide a higher-performance mechanical property, a wide variety of chemical components are added to pure HAp in the form of dopants. The ions used as the additives can replace Ca^{2+} , PO_4^{3-} , and OH^- ions within the crystal lattice of HAp, causing significant changes in the material's mechanical and biological properties [5, 10].

Er is a widely recognized rare-earth element. The human body contains Er with a higher concentration in rib bones and lower concentrations in the kidneys and liver [11, 12]. According to Gitty et al. [13], Er-doped HAp has potential

biphotonic advantages. Furthermore, due to its light emission spectra and outstanding biocompatibility, Er has been proposed as an appropriate dopant for HAp structures. In a separate work, Pham et al. [14], detailed the chemical precipitation-based synthesis of Er-doped HAp. Recent research has demonstrated that Gd-HAp exhibits favorable biocompatibility and a greater capacity for adsorbing proteins, suggesting that it may hold greater promise for prospective biological applications [15].

As was indicated earlier, there are a few publications on HAp that have been doped with Er^{3+} and Gd^{3+} , as the author mentioned above. However, to the best of our knowledge, there is no study that has been published on the impact of being Er, and Gd co-doped on the structure of HAp. The purpose of this investigation is to use the wet chemical route to produce HAp that has been co-doped with two types of heavy rare earth ions: erbium (Er^{3+}) and, gadolinium (Gd^{3+}) at constant amounts and to determine the effects of increasing amounts of glycerol used in the synthesis on structural properties of the Er/Gd co-doped HAp.

2. Material and Method

Calcium nitrate tetrahydrate (CN), gadolinium (III) nitrate hexahydrate (GN), erbium (III) nitrate pentahydrate (EN) and diammonium hydrogen phosphate (DAP) were used as the precursors of Ca, Gd, Er, and P, respectively. All the chemicals were obtained from Sigma-Aldrich. The distilled water was used as the dissolvent. 100 mL of 49.630 mmol CN, 0.185 mmol GN, and 0.185 mmol EN solution was prepared as the first mixture. 100 mL of 30.0 mmol of the DAP solution was prepared as the second mixture and poured drop wisely into the first mixture. The pH was adjusted to 10.0 by adding an ammonia solution (Sigma-Aldrich). After this step, different amounts (0, 4, 8, 12, and 16 mL) of glycerol (Sigma-Aldrich) were added to the final solution for each sample. The samples were named according to the amount of glycerol as G0, G4, G8, G12, and G16. The as-obtained mixture was stirred for 2 h at room temperature, dried in an oven at 120 °C for 90 h, and put in an electrical furnace at 900 °C for 1 h. After calcination, the HAp powders were produced.

The crystal structure characterization process was carried out using X-ray diffraction (XRD) measurements by the Bruker D8 Advance equipment. FTIR measurements were done using the Perkin Elmer Spectrum One spectrophotometer using the KBr method. Morphological observations were made using a scanning electron microscope (FEI Quanta 450 FEG).

3. Results and Discussions

3.1. XRD analysis

The XRD patterns shown in Fig. 1 point out the polycrystalline structure of the as-prepared HAp samples. A single phase of HAp (PDF No: 09–0432) is observed. No secondary phase is detected. The amount of the as-used glycerol causes some changes in the intensity and peak positions of the as-detected peaks.

The crystallite size (t) and crystallinity percent ($X_c\%$) were estimated by using the following Scherrer equation [16] and the relation reported by Landi et al. [17], respectively

$$t = \frac{0.9\lambda}{B_{1/2} \cos \theta} \quad (1)$$

$$X_c \% = \left(1 - \frac{V_{112/300}}{I_{300}}\right) \times 100 \quad (2)$$

where λ is the wavelength, θ is the diffraction angle, $B_{1/2}$ is the full width at half maximum, I_{300} is the intensity of the (300) peak, and $V_{112/300}$ is the intensity of the pit between the (112) and (300) diffraction peaks. The as-estimated values of the parameters calculated from the XRD patterns are given in Table 1. It is seen that both crystallite size and crystallinity percent of the glycerol-free sample (G0) are smaller than those of the glycerol-containing ones. Unit cell parameters are also affected by the glycerol content used in the synthesis.

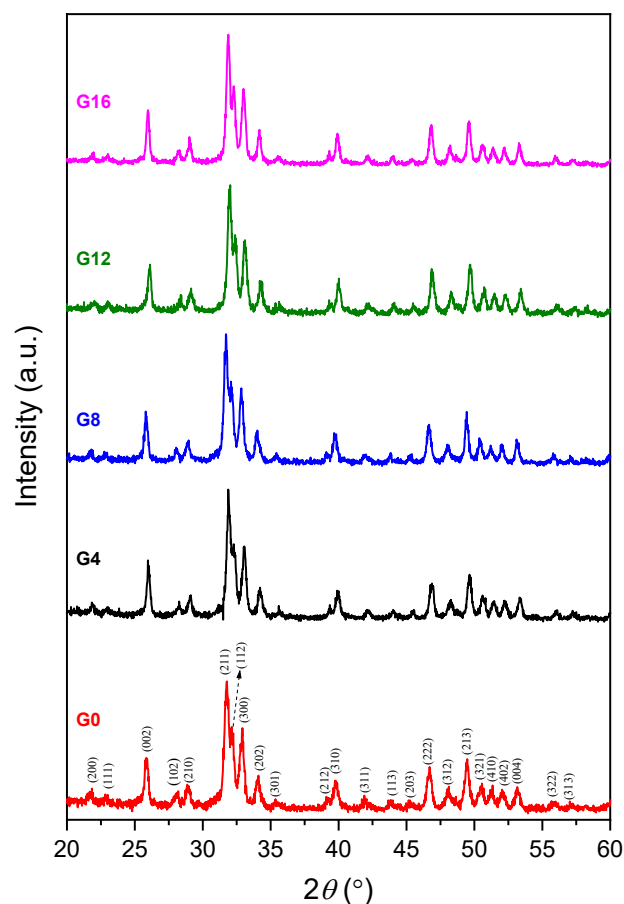


Fig. 1. XRD plots of the Er/Gd-based HAp

Table 1. XRD analysis results

Sample	<i>t</i> (nm)	<i>Xc</i> %	<i>a</i> (nm)	<i>c</i> (nm)	<i>c/a</i>	<i>V</i> (nm) ³
HAp*			0.9418	0.6884	0.7309	0.5288
G0	21.6	68.6	0.9418	0.6895	0.7321	0.5296
G4	24.1	74.2	0.9378	0.6854	0.7309	0.5220
G8	24.0	73.3	0.9440	0.6895	0.7304	0.5321
G12	23.0	72.4	0.9362	0.6818	0.7283	0.5175
G16	25.2	73.7	0.9395	0.6859	0.7301	0.5243

* represents the standard data reported in the JCPDS 09-0432 card.

3.2. FTIR spectroscopy results

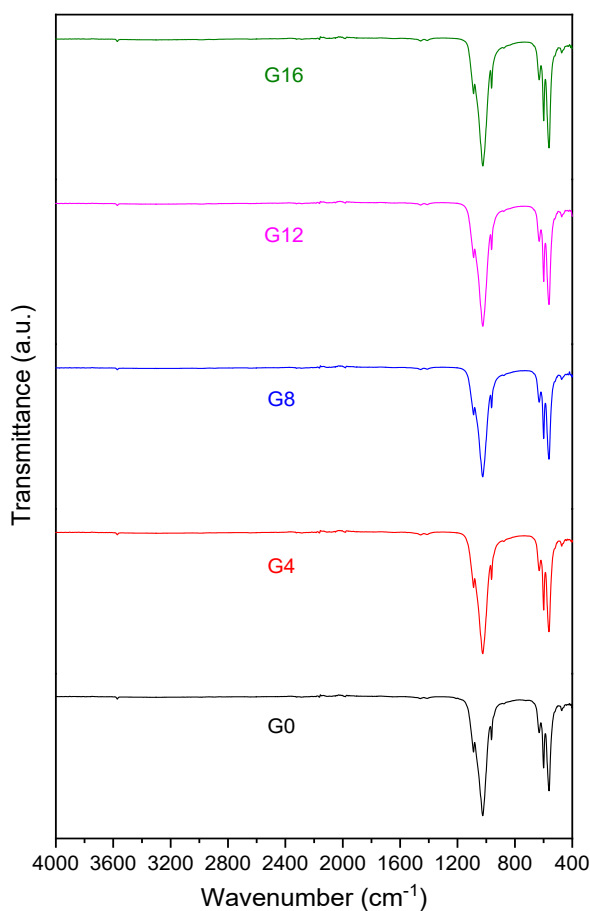


Fig. 2. FTIR results of the Er/Gd-based HAPs

The FTIR results shown in Fig. 2 reveal the functional groups found in the samples. In these spectra, the bands associated with hydroxyl and phosphate groups were detected in the spectral interval of 4000-400 cm^{-1} . The bands belonging to the vibrational modes of the hydroxyl group were observed at 631 (known as the libration mode) and 3572 cm^{-1} (stretching mode) [18]. The phosphate group-related bands were detected in these spectra at the band positions of 1088, 1023, 963, 600, 562, and 472 cm^{-1} . The bands detected at 1088 and 1023 cm^{-1} are related to the anti-symmetric stretching mode of the P-O bond [reference]. The sharp band, with the highest intensity

assigned to the symmetric stretching mode of the P-O bond was observed at 963 cm^{-1} [19]. The intense bands revealed detected at 600 and 562 cm^{-1} are associated with the bending mode of the O-P-O bond [20]. The weak band at 472 cm^{-1} is related to the bending mode of the phosphate group [21].

3.3. SEM observations

The SEM images taken at the magnification of X50,000 for all the samples are illustrated in Fig. 3. It is seen that all the samples are composed of smaller particles in nanosize. Compared to the glycerol-free sample (G0), the morphology is affected by the amount of the catalyst. In the EDX results, the elements of Ca, Er, Gd, P, and O are detected. The amount of Gd is found to be mostly higher than that of Er. It can be said that the penetration of Gd is greater than that of Er. The molar ratios of the (Ca+Gd+Er)/P are found to be 1.66, 1.62, 1.68, 1.71, and 1.68 for G0, G4, G8, G12, and G16, respectively.

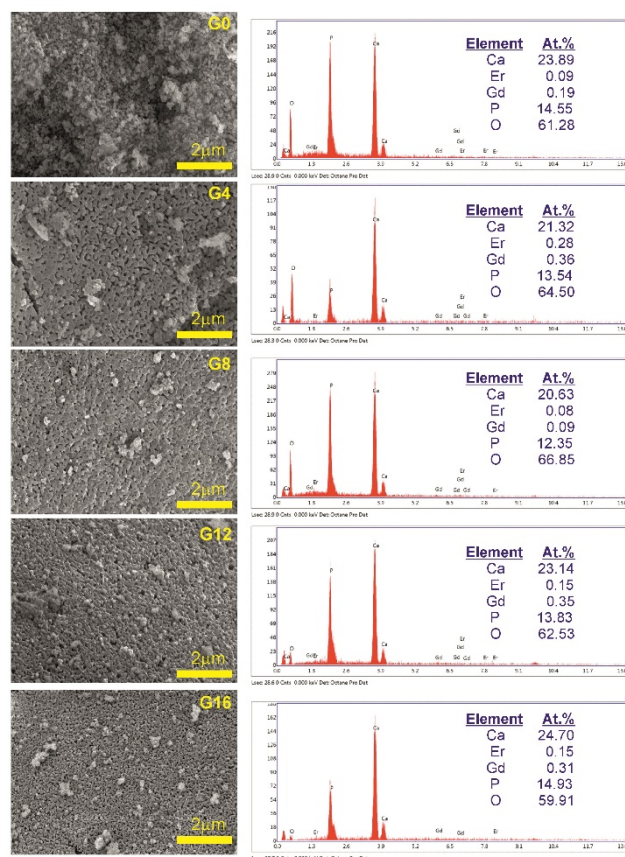


Fig. 3. SEM observations of the samples

4. Discussion

HAP samples co-doped with the same content of Er and Gd were prepared using a wet chemical method. The effects of the increasing glycerol used in the preparation of Er and Gd-based samples on their morphology and

structural properties were investigated. Significant effects of the glycerol catalyst on the as-investigated properties were observed. Higher crystallinity and crystallite size were found for the glycerol-containing HAP samples compared to the glycerol-free sample. It was found that Gd can have higher precipitation features in comparison to Er in the apatitic structure.

Competing interests

The authors declare that they have no competing interests.

Acknowledgments

This work was supported by the Management Unit of Scientific Research Projects of Firat University (FUBAP) (Projects No: FF.24.22 and MMY.24.03). This work was also supported by the Malatya Turgut Özal University Scientific Research Projects (BAP) Coordination Unit (Project No: 23H01).

References

- [1] R. Ghosh and R. Sarkar. Synthesis and characterization of sintered hydroxyapatite: a comparative study on the effect of preparation route. *Journal of the Australian Ceramic Society*. 2018;54:71-80. <https://doi.org/10.1007/s41779-017-0128-5>.
- [2] S.V. Dorozhkin. Calcium orthophosphates: occurrence, properties, biomineralization, pathological calcification and biomimetic applications. *Biomater*. 2011;1(2):121-164. <https://doi.org/10.4161/biom.18790>.
- [3] O. Kaygili, S. Keser, T. Ates, A.A. Al-Ghamdi and F. Yakuphanoglu. Controlling of dielectrical and optical properties of hydroxyapatite based bioceramics by Cd content. *Powder technology*. 2013;245:1-6. <https://doi.org/10.1016/j.powtec.2013.04.012>.
- [4] R.O. Kareem, N. Bulut and O. Kaygili. Hydroxyapatite biomaterials: a comprehensive review of their properties, structures, medical applications, and fabrication methods. *Journal of Chemical Reviews*. 2024;6(1):1-26. <https://doi.org/10.48309/JCR.2024.415051.1253>.
- [5] A.A. Korkmaz, L.O. Ahmed, R.O. Kareem, H. Kebiroglu, T. Ates, N. Bulut, O. Kaygili and B. Ates. Theoretical and experimental characterization of Sn-based hydroxyapatites doped with Bi. *Journal of the Australian Ceramic Society*. 2022;58:803-815. <https://doi.org/10.1007/s41779-022-00730-5>.
- [6] N. Bulut, O. Kaygili, A.H. Hssain, S.V. Dorozhkin, B. Abdelghani, C. Orek, H. Kebiroglu, T. Ates and R.O. Kareem. Mg-Dopant Effects on Band Structures of Zn-Based Hydroxyapatites: A Theoretical Study. *Iranian Journal of Science*. 2023;47:1843-1859. <https://doi.org/10.1007/s40995-023-01531-6>.
- [7] M. Sadat-Shojai, M.-T. Khorasani, E. Dinpanah-Khoshdargi and A. Jamshidi. Synthesis methods for nanosized hydroxyapatite with diverse structures. *Acta biomaterialia*. 2013;9(8):7591-7621. <https://doi.org/10.1016/j.actbio.2013.04.012>.
- [8] V. Putlayev, P. Evdokimov, A. Garshev, D. Prosvirin, E. Klimashina, T. Safronova and V. Ivanov. Strength characteristics of resorbable osteoconductive ceramics based on diphosphates of calcium and alkali metals. *Russian Physics Journal*. 2014;56:1183-1189. <https://doi.org/10.1007/s11182-014-0160-7>.
- [9] R.O. Kareem, O. Kaygili, T. Ates, N. Bulut, S. Koytepe, A. Kuruçay, F. Ercan and I. Ercan. Experimental and theoretical characterization of Bi-based hydroxyapatites doped with Ce. *Ceramics International*. 2022;48(22):33440-33454. <https://doi.org/10.1016/j.ceramint.2022.07.287>.
- [10] M. Othmani, H. Bachoua, Y. Ghandour, A. Aissa and M. Debbabi. Synthesis, characterization and catalytic properties of copper-substituted hydroxyapatite nanocrystals. *Materials Research Bulletin*. 2018;97:560-566. <https://doi.org/10.1016/j.materresbull.2017.09.056>.
- [11] S. Zaichick, V. Zaichick, V. Karandashev and S. Nosenko. Accumulation of rare earth elements in human bone within the lifespan. *Metallomics*. 2011;3(2):186-194. <https://doi.org/10.1039/c0mt00069h>.
- [12] B.K. Mahmood, O. Kaygili, N. Bulut, S.V. Dorozhkin, T. Ates, S. Koytepe, C. Gürses, F. Ercan, H. Kebiroglu, R.S. Agid and T. İnce. Effects of strontium-erbium co-doping on the structural properties of hydroxyapatite: An Experimental and theoretical study. *Ceramics International*. 2020;46(10B):16354-16363. <https://doi.org/10.1016/j.ceramint.2020.03.194>.
- [13] P. Gitty, M. Kailasnath and V.P. Nampoori. Synthesis, structure and luminescence characterization of erbium doped hydroxyapatite nanoparticles by precipitation method. *Current Physical Chemistry*. 2019;9(3):218-225. <https://doi.org/10.2174/1877946809666190708124928>.
- [14] V.-H. Pham, H.N. Van, P.D. Tam and H.N.T. Ha. A novel 1540 nm light emission from erbium doped hydroxyapatite/ β -tricalcium phosphate through co-precipitation method. *Materials Letters*. 2016;167:145-147. <https://doi.org/10.1016/j.matlet.2016.01.002>.
- [15] S.-j. Yuan, X.-y. Qi, H. Zhang, L. Yuan and J. Huang. Doping gadolinium versus lanthanum into hydroxyapatite particles for better biocompatibility in bone marrow stem cells. *Chemico-Biological Interactions*. 2021;346:109579. <https://doi.org/10.1016/j.cbi.2021.109579>.
- [16] B. D. Cullity. *Elements of X-ray Diffraction*, Addison, Wesley Mass: 1978. p. 127–131.
- [17] E. Landi, A. Tampieri, G. Celotti and S. Sprio. Densification behaviour and mechanisms of synthetic hydroxyapatites. *Journal of the European Ceramic Society*. 2000;20(14-15):2377–2387. [https://doi.org/10.1016/s0955-2219\(00\)00154-0](https://doi.org/10.1016/s0955-2219(00)00154-0).
- [18] M.A. Goldberg, P.V. Protsenko, V.V. Smirnov, O.S. Antonova, S.V. Smirnov, A.A. Kononov, K.G. Vorckachev, E.A. Kudryavtsev, S.M. Barinov and V.S. Komlev. The enhancement of hydroxyapatite thermal stability by Al doping. *Journal of Materials Research and Technology*. 2020;9(1):76-88. <https://doi.org/10.1016/j.jmrt.2019.10.032>.
- [19] Z. Hong, S. Wang and F. Liu. Synthesis of Tubular Hydroxyapatite and Its Application in Polycaprolactone Scaffold Materials. *Journal of Functional Biomaterials*. 2024;15(1):22. <https://doi.org/10.3390/jfb15010022>.
- [20] M.W. Teoh, C.K. Ng, S.K.Y. Lee, S. Ramesh, C.H. Ting, Y.D. Chuah, I.Y. Lim, C.Y. Tan and U. Sutharsini. Densification behaviors of hydroxyapatite/pectin bio-ceramics. *Materials Today: Proceedings*. (In Press) 2023. <https://doi.org/10.1016/j.matpr.2023.04.388>.
- [21] M. L. Habib, S.A. Disha, M.S. Hossain, M.N. Uddin and S. Ahmed. Enhancement of antimicrobial properties by metals

doping in nano-crystalline hydroxyapatite for efficient biomedical applications. *Heliyon*. 2024;10(1):e23845. <https://doi.org/10.1016/j.heliyon.2023.e23845>.